

Original Research Article

Covalent Immobilization of *Myrothecium verrucaria* Bilirubin Oxidase onto Polypyrrole Nanoparticles and Polyaniline Composite Film for Amperometric Detection of Serum Bilirubin

Bhawna Batra, Namita Malik and C.S.Pundir*

Department of Biochemistry, M.D.University, Rohtak-124 001, India

*Corresponding author

ABSTRACT

A *Myrothecium verrucaria* bilirubin oxidase (BOx) has been immobilized covalently onto polypyrrole nanoparticles (PPyNPs) and polyaniline (PANI) nanocomposite film, electrodeposited onto Au electrode. The enzyme electrode was characterized by scanning electron microscopy (SEM), Fourier transform infrared spectroscopy (FTIR), electrochemical impedance spectroscopy (EIS) and cyclic voltammetry (CV). An amperometric bilirubin biosensor was fabricated by connecting this enzyme electrode with the Ag/AgCl reference electrode and Pt wire as auxiliary electrode through potentiostat. The biosensor showed optimum response within 2s at pH 9.0 (0.1 mol/L Tris-HCl) and 36°C, when operated at -0.16V. The biosensor exhibited excellent sensitivity (detection limit as 0.1 μmol/L), fast response time and wider linear/working range (from 0.01 to 320 μmol/L). Analytical recovery of added bilirubin was 97.91–98.47% and within batch and between batch coefficients of variation were 5.04% and 5.40% respectively. There was a good correlation between serum bilirubin values obtained by standard colorimetric method and the present method ($r = 0.97$). The biosensor was employed to measure bilirubin levels in sera of apparently healthy persons and persons suffering from jaundice. The enzyme electrode lost 20% of its initial activity after 60 days of its regular uses, when stored dry at 4°C.

Keywords

Myrothecium verrucaria,
Bilirubin oxidase,
Bilirubin,
Polypyrrole nanoparticles,
Polyaniline,
Serum

Introduction

Bilirubin, a water-insoluble tetrapyrrole compound and yellow colored principal pigment in bile, is the metabolic product of normal heme catabolism, present in the blood in an unconjugated (free) form (Malhotra and Chaubey, 2003). After it circulates through the liver, it is transformed to a water-soluble conjugated form and

finally excreted into bile. As an index of liver function, serum bilirubin levels indicate how well the liver is processing bilirubin and help in diagnosis and prediction of haemolytic disorders in adults as well as in newborn infants (Sherwin and Obernolte, 1989). The determination of serum bilirubin is of great importance for

the differential diagnosis of jaundice. Clinically hyperbilirubinemia appears as jaundice or icterus. Jaundice can usually be detected, when the serum bilirubin level exceeds 2.0 to 2.5 mg/dL. However, unconjugated plasma bilirubin that is not bound to albumin, can cross the blood brain barrier. In conditions such as neonatal jaundice or crigler-najjar syndrome, extremely high concentrations > 3.42 mmol/L of unconjugated bilirubin can accumulate and the resulting diffusion of bilirubin into the central nervous system can cause encephalopathy and permanent impairment of nervous function. Higher levels of bilirubin may lead to brain damage or even death in case of newborns (Maisels, 2009).

Various methods have been developed for determination of bilirubin in clinical samples, the most common being the direct spectroscopic measurement (Doumas et al., 1973) and the diazo reaction method (Bregmeyer et al., 1985). Quantification of the bilirubin with this method is also compromised, partly as the reaction rate is pH dependent (Li and Rosenzweig, 1997). Other analytical methods for bilirubin determination such as polarography (Koch and Oakingbe, 1981), and fluorometry (Wang and Ozsoz, 1990) require costly equipment, time consuming sample preparation and skilled persons to operate, and thus are not suitable for routine. Extensive attempts have been made to obtain more accurate and simple analytical methods including various enzymatic systems and biosensors for the determination of bilirubin for a large number of clinical samples. Nevertheless, biosensing methods are comparatively more simple, rapid and sensitive than the existing methods and require no sample pre-treatment. Electrochemical amperometric bilirubin biosensors employing bilirubin

oxidase (BOx) are based on either the measurement of decreasing level of molecular oxygen (Fortuney and Guilbault, 1996) or electrochemical oxidation of hydrogen peroxide (Rahmana et al., 2008) or the mediated electron transfer by the Mn (II) ion using a conductive poly-terthiophene-Mn (II) complex (Wang, 2005).

In recent years, a wide variety of nanoparticles with special properties have found broad application in biosensors. Because of their small physical size, nanoparticles present unique chemical, physical and electronic properties that are different from those of bulk materials (Zhao and Jiang, 2010) and improved new biosensors have been designed benefiting from these novel attributes. Now a days, nanoparticles-enhanced biosensors show significant development. Polypyrrole (PPy) as an excellent conducting polymer, plays an important role in the electrochemical biosensors to achieve their increased electrochemical activity and sensitivity, owing to its good biocompatibility, conductivity, stability, and efficient polymerization at neutral pH as well as easy synthesis (Reung-u-Rai et al., 2008).

Highly conductive PPy nanoparticles of diameter ranging from 60-90 nm can be synthesized by the microemulsion polymerization of pyrrole (Tiwari et al., 2007). Polyaniline (PANI) is one of the conducting polymers known for transducing support in biosensors, because of its properties like high conductivity, low cost, relatively high stability and facile production by electrodeposition (Teles and Fonseca, 2008). Electrochemical biosensing is among the most promising applications of PANI (Michira et al., 2007). PANI has ability to immobilize and provide direct electrical communication between the enzyme and electrode in amperometric

biosensors (Bais et al., 1980). PANI-modified electrodes render very high signal amplification and prevent electrode fouling. The present work describes a unique approach of immobilizing bilirubin oxidase onto PPyNPs/PANI, modified Au electrode and its application in construction of an amperometric biosensor for determination of bilirubin, which is expected to provide high sensitivity, high biocompatibility, high charge transfer rate and good stability.

Experiment section

Materials

Bilirubin oxidase (BOx) from *Myrothecium verrucaria* and sodium dodecyl sulphate (SDS) from Sigma-Aldrich, St.Louis, USA, polyaniline from Spectrochem Pvt. Ltd. Mumbai, India; pyrrole, ammonium peroxy disulphate (APS), glycine, acetonitril, acetic acid, sodium hydroxide, potassium ferrocyanide, potassium ferricyanide, silica gel, N-hydroxy succinimide (NHS) and potassium chloride (KCl), from SISCO Research Lab, Mumbai, India, sulphuric acid from Qualigens Fine Chemicals, Mumbai, India were used. Double distilled water (DW) was used throughout the experimental studies.

Apparatus

Potentiostat/Galvanostat (Make: Autolab, model: AUT83785, manufactured by Eco Chemie) with a three electrode system consisting of a Pt wire as an auxiliary electrode, an Ag/AgCl electrode as reference electrode and BOx/PPy NPs/PANI modified Au electrode as a working electrode. Scanning electron microscope (SEM) (Zeiss EV040). UV Spectrophotometer (Make: Shimadzu, Model 1700), X-ray diffractometer (XRD), (Make: 122 Rigaku, D/Max2550, Tokyo, Japan), Fourier transform Infra-red spectrometer (FTIR)

(Thermo Scientific, USA).

Assay of free bilirubin oxidase (BOx)

The assay of free BOx was carried out and that was based on the quantification of H₂O₂, generated from oxidation of bilirubin catalyzed by bilirubin oxidase, using a color reaction consisting of 4-aminophenazone, phenol and peroxidase as chromogenic system (Klemm et al., 2000). The reaction mixture containing 1.8 ml of Tris HCl buffer pH 8.5 (0.2 mol/L), 0.1 ml of bilirubin solution (34.21 micro mol/L), 0.1 mL of BOx solution (5 U/mL) was incubated at 37 °C for 10 min. One mL of colour reagent was added and incubated it in dark at 37 °C for 15 min to develop the color, A₅₂₀ was read and H₂O₂ concentration was extrapolated from its standard curve.

One unit of enzyme is defined as amount of enzyme required to catalyze the formation of 1.0 nmole of H₂O₂ from oxidation of bilirubin per min/ ml under standard assay conditions.

Preparation of PPyNPs

PPyNPs were synthesized by microemulsion polymerization of pyrrole and ammonium peroxydisulfate (APS) in the presence of surfactant dopants (Tiwari et al., 2007). Dopant used was sodium dodecyl sulphate (SDS). Aqueous solution of 0.08 M SDS was made and stirred vigorously for 20 minutes followed by addition of pyrrole (0.08 mol/L) and further stirring for 30 minutes. APS (0.08 mol/L) was added and the solution was frozen for 24 hours. Excessive methanol was added to terminate the reaction. Mixture was centrifuged at 5000 rpm for 15 min. Precipitate was washed with methanol and DW and was filtered. PpyNps were obtained and the prepared nanoparticles were kept at 40 °C for drying.

FTIR of PPy nanoparticles

FTIR-Fourier Transform Infra-red Spectroscopy is the chemically specific analysis technique used to identify chemical compounds and substituent groups and the resulting spectrum represents the molecular absorption and transmission, creating a molecular fingerprint of the sample. FTIR of PPy nanoparticles was carried out using KBr as reference pellet against the pellet of Polypyrrole.

Electrodeposition of PPyNPs/PANI onto gold electrode

The surface of Au electrode (2cm × 1 mm) was polished manually by alumina slurry (diameter 0.05 μm) with a polishing cloth, followed by thorough washing with DW and then placed into ethanol, sonicated to remove adsorbed particles and finally washed with DW for 3-4 times. 200 μl aniline (10.9 mol/L) was added into 25 mL of 1 mol/L acetonitrile to achieve its final concentration as 0.08 mol/L and electropolymerized onto surface of Au electrode through cyclic voltammetry in a Potentiostat-Galvanostat (Make: Autolab, model: AUT83785, manufactured by Eco Chemie, The Netherland) to reach 20th polymerization cycle at - 0.3 to 0.7 V. PPyNPs suspension (200 μl) was added to this 25 mL of 1 mol/L of acetonitrile to reach 20th deposition cycle at -0.3 to 0.7 V at a scan rate of 20 mVs⁻¹ (Fig.1). The resulting PPyNPs/PANI modified Au electrode was washed thoroughly with DW to remove unbound matter and kept in a dry petri-plate at 4 °C.

Immobilization of BOx onto PPyNPs/PANI modified Au electrode

PPyNPs/PANI/Au electrode was dipped into

1 ml of 2.5% glutaraldehyde and EDC+NHS in 0.1 mol/L Tris HCl buffer, pH 9.0 and kept at room temperature for 7 h, washed thoroughly in DW and dipped into 1.5 mL of BOx solution (5 U/mL) and kept overnight at room temperature for immobilization. The resulting electrode with immobilized BOx was washed 3-4 times with 0.1 mol/L Tris HCl buffer, pH 9.0 to remove residual unbound protein. The resulting BOx/PPyNPs/PANI/Au electrode was used as working electrode and stored at 4°C when not in use. This working electrode was characterized by SEM at different stages of its construction.

Cyclic voltametry measurement and testing of bilirubin biosensor

Cyclic voltametry (CV) of BOx/PPyNPs/PANI/Au electrode was recorded in Potentiostat-Galvanostat from -0.05 to 0.5V Vs Ag/AgCl as reference and Pt wire as counter electrode in a 25 ml of 0.2 mol/L Tris HCl buffer (pH 9.0) containing 100 μl of 34.21 μmol/L bilirubin.

Optimization of bilirubin biosensor

To optimize working conditions of the biosensor, effects of pH, incubation temperature, time and substrate (bilirubin) concentration on biosensor response were studied. To determine optimum pH, the pH was varied between pH 5.5 to 10.0 at an interval of pH 0.5 using the following buffer, each at a final concentration of 0.1 mol/L: pH 5.5 to 7.5 sodium phosphate buffers, pH 8.5 to 9.0 Tris HCl buffer and pH 9.5 to 10 glycine buffer. Similarly to determine optimum temperature the reaction mixture was incubated at different temperature (20–50°C). The effect of bilirubin concentration on biosensor response was determined by varying the concentration of bilirubin in the range

0.014-375 $\mu\text{mol/L}$.

Application of bilirubin biosensor in sera

Blood samples (1 mL each) were drawn from apparently healthy male and female (20 each) and persons having a diagnosis of jaundice at Pt. BDS PGIMS, Rohtak hospital and centrifuged at 2000 r.p.m. for 10–15 min and their supernatant (serum) was collected. Bilirubin content in serum was determined by the present biosensor in the similar manner as described above for its response measurement, under its optimal working conditions except that bilirubin was replaced by serum sample. The bilirubin content in serum was interpolated from standard curve between bilirubin concentration versus current in mA prepared under optimal assay conditions of BOx/PPy NPs/PANI/Au electrode using straight line equation $y=mx+c$ (Fig.2).

Storage stability of BOx/PPyNPs/PANI/Au electrode

The stability of the working electrode was studied for 2 months by performing the assay on weekly basis. The present electrode system was stored in dried condition at 4 °C when not in use.

Results and Discussion

Characterization of PPyNPs

Polypyrrole nanoparticles were characterized by recording their UV and visible spectra in a UV-visible spectrophotometer, X-ray diffraction pattern in a X-ray diffractometer (XRD) and fourier transform Infra-red spectrometer (FTIR) (Fig. 3). UV and visible spectra exhibited strong absorbance peak at 440 nm (Fig. 3 A), confirming high degree of conductivity and doping and hence the synthesis of PPyNPs. The XRD patterns of the prepared NPs clearly showed the characteristic peak

of PPyNPs (Fig. 3 B). No characteristic peaks of impurities were observed, revealing the high purity of the PPyNPs. The typical TEM images of PPyNPs nanoparticles showed the spherical shape of PPy nanoparticles with an average size of 60 – 90 nm in diameter (Fig. 3 C). FTIR spectra of the PPy nanoparticles synthesized by microemulsion polymerization indicated the typical characteristics of PPy which were consistent with literature (Tiwari et al., 2007). The peaks at 1548 and 1470 cm^{-1} correspond to the stretching vibration of C=C and C-N of PPy respectively. The peak at 1196 cm^{-1} is attributed to vibration of the pyrrole ring (Fig. 3 D)

SEM studies of gold electrode during its modification

The SEM images of the surface of bare gold electrode, PPyNPs/PANI/Au electrode and BOx/PPyNPs/PANI/Au electrode are shown in Fig. 4 respectively. The stepwise modification of electrode could be seen clearly from these SEM images. The SEM image of the PPyNPs/PANI/Au composite film exhibited a net structure. Film is more uniform and porous (Fig. 4 a) hence effective surface area is larger. On immobilization of BOx, the globular structural morphology appears due to the covalent interaction between PPyNPs/PANI/Au electrode with BOx (Fig. 4 b).

FTIR spectra

Fig.5. showed FTIR spectra of PANI/Au electrode (curve i), PPyNPs/PANI/Au electrode (curve ii) and BOx/PPyNPs/PANI/Au electrode (curve iii). FTIR spectra of electrodeposited PANI/Au showed a band at 3000 cm^{-1} due to N–H stretching of the benzenoid ring. The peak at 1510 cm^{-1} is assigned to the quinonoid ring and 1492 cm^{-1} is attributed to the benzoid

ring (curve i). FTIR spectra of deposited PPyNPs/PANI/Au electrode showed bands at 1550 and 1475 cm^{-1} correspond to the stretching vibration of C=C and C-N of PPy respectively. The peak at 1190 cm^{-1} is attributed to breathing vibration of the pyrrole ring. The bands of C-H and N-H in-plane deformation vibration are located at 1037 cm^{-1} while the band of C-H out-of-plane deformation vibration are found at 901 cm^{-1} at 1360 and 3398 cm^{-1} due to the presence of C-N bending and N-H stretching vibrations, respectively (curve ii). The peak at 1762 cm^{-1} is assigned to C-O stretching, while peak at 1549 cm^{-1} is attributed to amide I group (C-O stretching along with N-H deformation mode) as shown in curve iii. This shows the covalent immobilization of BOx onto PPyNPs/PANI/Au electrode.

Electrochemical impedance measurements (EIS)

Fig. 6 showed electrochemical impedance spectra (EIS) of (i) bare Au electrode (ii) PPyNPs/PANI/Au electrode and (iii) BOx/PPyNPs/PANI/Au electrode in containing 5 mM $\text{K}_3\text{Fe}(\text{CN})_6/\text{K}_4\text{Fe}(\text{CN})_6$ (1:1) as a redox probe. EIS provided an effective method to probe electronic features of surface-modified electrodes.

The R_{CT} values (semicircle diameter) for bare Au electrode, PPyNPs/PANI/Au electrode and BOx/PPyNPs/PANI/Au electrodes were 970 Ω , 650 Ω and 757 Ω respectively. The R_{CT} of BOx/PPyNPs/PANI/Au (iii) bioelectrode was higher compared with that of PPyNPs/PANI/Au (ii) electrode. This increase in R_{CT} can be attributed to the fact that most biological molecules, including enzymes, are poor electrical conductors and cause hindrance to electron transfer. These results also indicate the binding of enzymes onto PPyNPs/PANI/Au composite.

Construction of bilirubin biosensor

A schematic representation of the construction of enzyme electrode based on covalent immobilization of BOx on PPyNPs decorated PANI film electrodeposited onto surface of Au electrode is shown in Fig. 7. PANI and PPyNPs were co-electropolymerised on the surface of Au electrode. Layer thickness could be easily controlled in this method. To construct the enzyme electrode, BOx was immobilized covalently onto PPyNPs/PANI/Au electrode through glutaraldehyde coupling. One -CHO group of glutaraldehyde was linked to -NH₂ group on surface of enzyme, while other -CHO group was bound to -NH₂ group of PANI on PPyNPs-PANI composite film, which provided physically more stable complex. The CVs of PPyNPs/PANI/Au exhibited higher currents than PANI/Au revealing that PPyNPs/PANI/Au composite film has large effective surface area than PANI/Au composite film and PPyNPs/PANI/Au composite film could provide a conducting path through the composite matrix for faster kinetics. Hence PPyNPs acting as electron transfer mediator help in enhancing the biosensor response and thus increases its sensitivity. The CV for Au, BOx/PANI/Au & BOx/PPyNPs/PANI/Au electrode was recorded. Au electrode showed no peak. Both the BOx electrodes showed current peak which was higher in case of BOx/PPyNPs/PANI/Au than that of BOx/PANI/Au which might be due to an increase in surface area as well as conductivity because of PPyNPs (Fig. 8). It has been reported that polypyrrole nanoparticles (PPyNPs) can be effectively dispersed due to large surface area for reactions and highly porous in sol form, hence PPyNPs provide good conductivity (Reung-u-Rai et al., 2008).

Response measurements of bilirubin biosensor

The optimum response was obtained at -0.16V and measured in terms of maximum current achieved in milli-amperes (mA) (Fig. 9) and hence subsequent studies were carried out at this voltage.

Optimization of Biosensor

The optimum current was obtained at pH 9.0 which is almost similar to that of bilirubin biosensor covalent immobilization of bilirubin oxidase onto zirconia coated silica nanoparticles/chitosan hybrid film (pH 8.5) (Wang et al., 2009) but higher than a conductive poly-terthiophene-Mn(II) complex (pH 7.0) (Rahmana et al., 2008) glassy carbon modified with ferrocenecarboxamide, gold nanoparticles and multiwall carbon nanotubes (pH 8.0) (Wang et al., 2009). At pH 9.0, it is the synergistic effect of both PPyNPs and PANI but not of PANI alone which is enough to promote electron transfer, the low conductivity of PANI at pH 9.0 could be compensated by highly conducting PPyNPs. The response was found to be increased as the temperature increased from 15-40 °C. The optimum temperature of the bilirubin oxidase biosensor was observed at 36 °C. The current response decreased rapidly after 36-50°C due to thermal inactivation of the enzyme. Hence, the subsequent experiments were performed at 36°C. There was a hyperbolic relationship between biosensor response and bilirubin concentration in the range, 0.014-320 µmol/L, the response was constant after 320 µmol/L.

Evaluation of biosensor

Linearity

There was a linear relationship between the current (in µA) and the bilirubin

concentration in the range 0.014-320 µmol/L, which is wider than reported earlier (Yang and Zhang, 2011) (0.0–80 µmol/L).

Detection limit

The detection limit of the present sensor was 0.01µmol/L, which is almost equal to that of earlier biosensor based on the modification of molecularly imprinted hydroxyapatite (HAP) film onto a quartz crystal by molecular imprinting and surface sol-gel technique. (0.01 µmol/L) (Yang and Zhang, 2011).

Analytical recovery

The average recoveries of bilirubin added to blood serum (at levels of 5 mmol/L and 10 mmol/L) were 98.5 and 97.9% demonstrating the satisfactory reliability of the present biosensor.

Precision

Within-sample and between-sample coefficients of variation for the determination of bilirubin in serum on the same day and after one week of storage were 5.04 and 5.40%, respectively. These high precisions highlight the good reproducibility and consistency of the present method, which can be attributed to the covalent immobilization of BOx onto the PPyNPs/PANI/Au electrode.

Application of bilirubin biosensor

The bilirubin level in human serum as measured by the current biosensor was in the range of 0.01 to 320 µmol/L. When these results were compared with those obtained by the standard chemical/ photo colorimetric method, there was a good correlation ($r = 0.972$) (Fig. 10). The comparative results obtained in the present study on sera bilirubin of healthy persons and jaundiced persons are summarized in Table 1.

Table.1 Serum bilirubin levels in apparently healthy persons and jaundice patients, as measured by bilirubin biosensor based on bilirubin oxidase PPyNPs/PANI/Au composite film

Sex	Age	Healthy Persons (μM) Mean ± SD	Sex	Age	Jaundice patients (μM) Mean ± SD
M	15	19 ± 0.4	M	29	29 ± 0.4
M	17	11 ± 0.5	M	32	44 ± 0.2
M	18	20 ± 0.5	M	39	25 ± 0.2
M	22	12 ± 0.3	M	42	28 ± 0.4
M	26	18 ± 0.3	M	45	52 ± 0.2
M	29	19 ± 0.1	M	46	30 ± 0.2
M	32	13 ± 0.3	M	46	49 ± 0.3
M	33	17 ± 0.2	M	49	42 ± 0.1
M	41	09 ± 0.4	M	52	45 ± 0.4
M	54	16 ± 0.5	M	52	43 ± 0.5
M	55	09 ± 0.3	F	09	27 ± 0.6
F	09	06 ± 0.5	F	10	22 ± 0.4
F	12	11 ± 0.5	F	16	28 ± 0.1
F	12	04 ± 0.1	F	17	24 ± 0.3
F	14	20 ± 0.4	F	17	33 ± 0.2
F	24	20 ± 0.4	F	24	26 ± 0.2
F	25	13 ± 0.06	F	35	21 ± 0.5
F	27	14 ± 0.02	F	54	39 ± 0.6
F	33	17 ± 0.02	F	54	36 ± 0.3
F	38	07 ± 0.05	F	60	43 ± 0.4

Fig.1 Cyclic voltamogram for electrodeposition of PPyNPs/PANI composite film. Supporting electrolyte: 1M acetonitrile solution; Scan rate: 20 mV/s

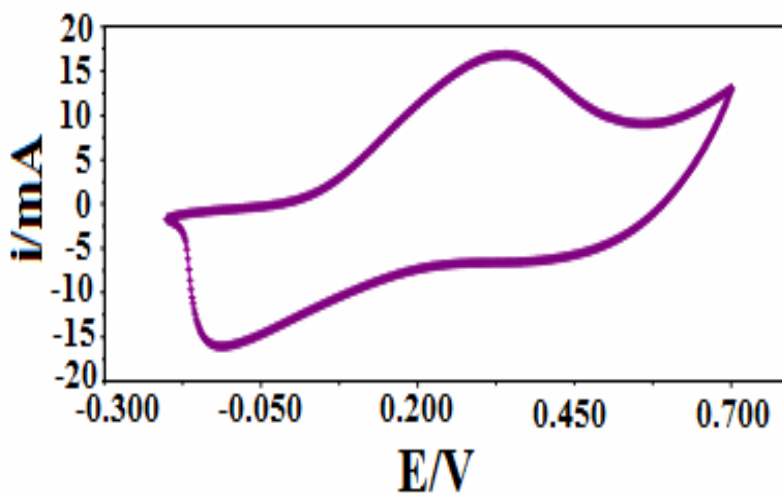


Fig.2 Standard curve for bilirubin biosensor for effect of bilirubin concentration on response of bilirubin biosensor based on PPyNPs/PANI/Au electrode bound bilirubin oxidase

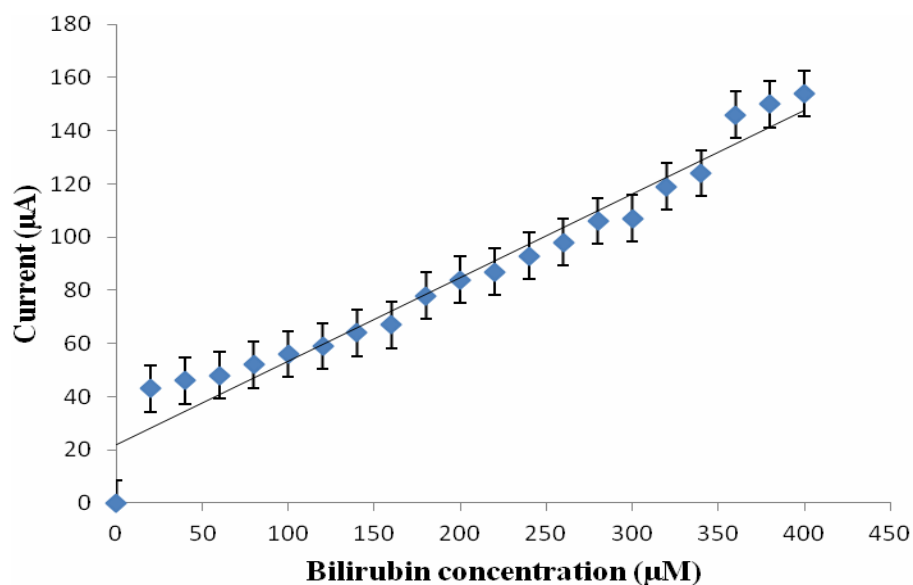


Fig.3 (A) UV-visible spectra of PPyNPs/PANI (B) X-ray diffraction (XRD) pattern of PPyNPs/PANI (C) Transmission electron microscopic (TEM) image of PPyNPs/PANI (D) FTIR spectra of PPyNPs

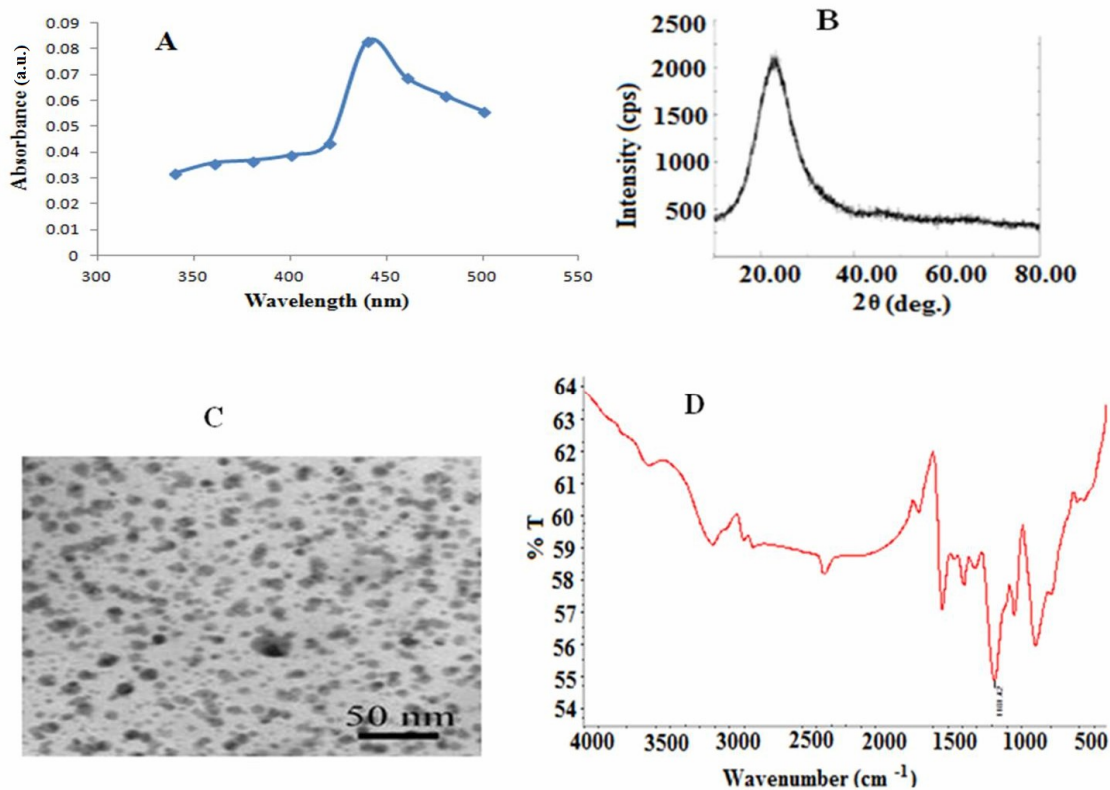


Fig.4 SEM images of (a) PPyNPs/PANI/Au electrode (b) BOx/PPyNPs/PANI/Au electrode

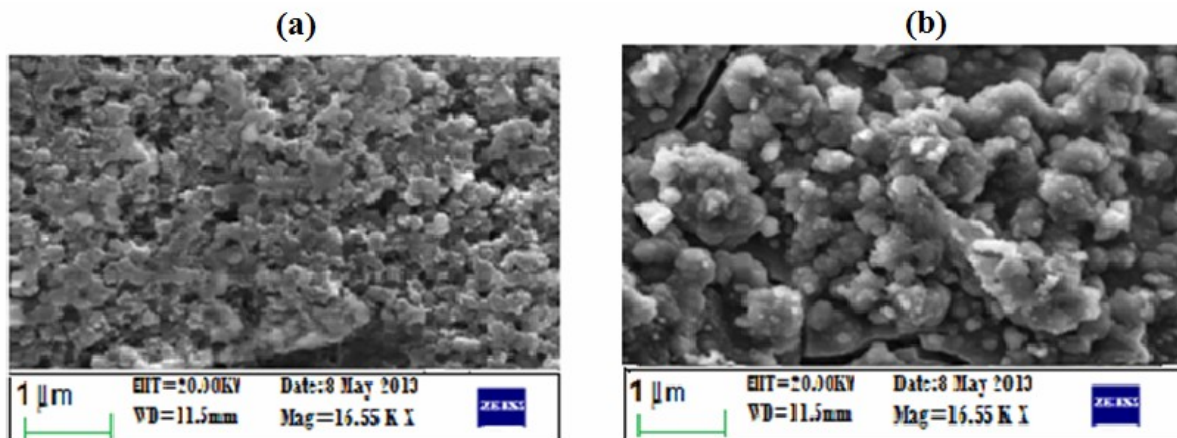


Fig.5 FTIR spectra of (i) PANI/Au electrode (ii) PPyNPs/PANI/Au electrode (iii) BOx/PPyNPs/PANI/Au electrode

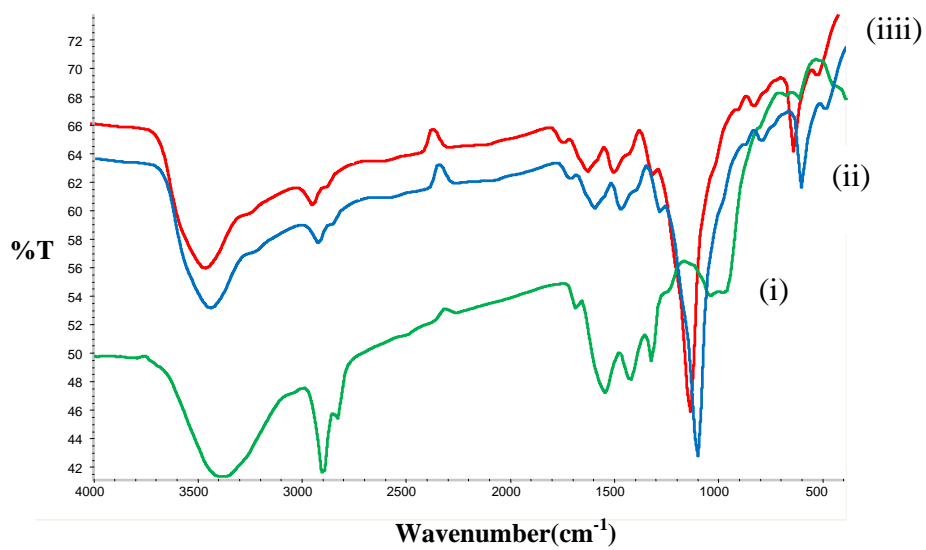


Fig.6 Impedance spectroscopy study of (i) Bare Au (ii) PPyNPs/PANI/Au (iii) BOx/PPyNPs/PANI/Au in 5 mM $K_3Fe(CN)_6/K_4Fe(CN)_6$ (1:1) as a redox probe

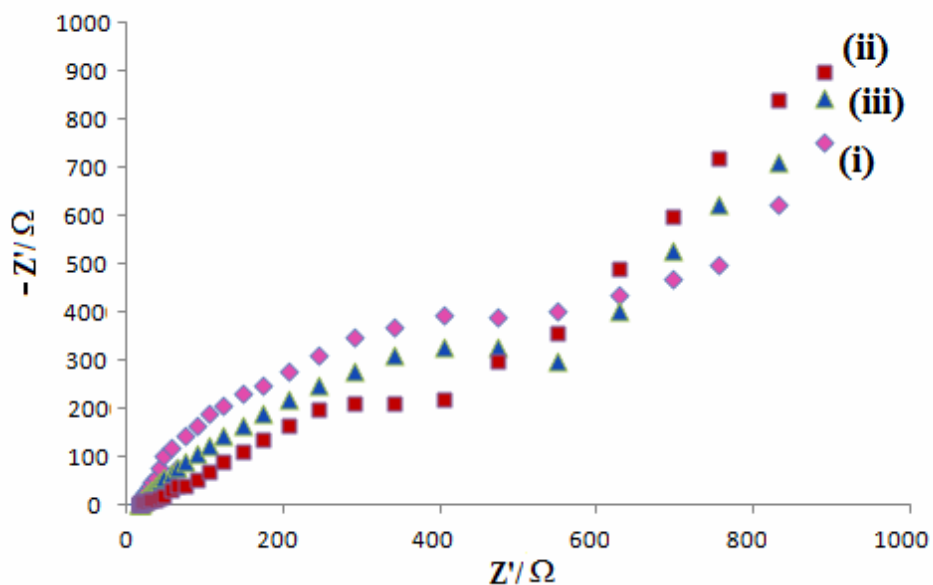


Fig.7 Schematic representation of chemical reaction involved in the fabrication of BOx/PPyNPs/PANI/Au electrode

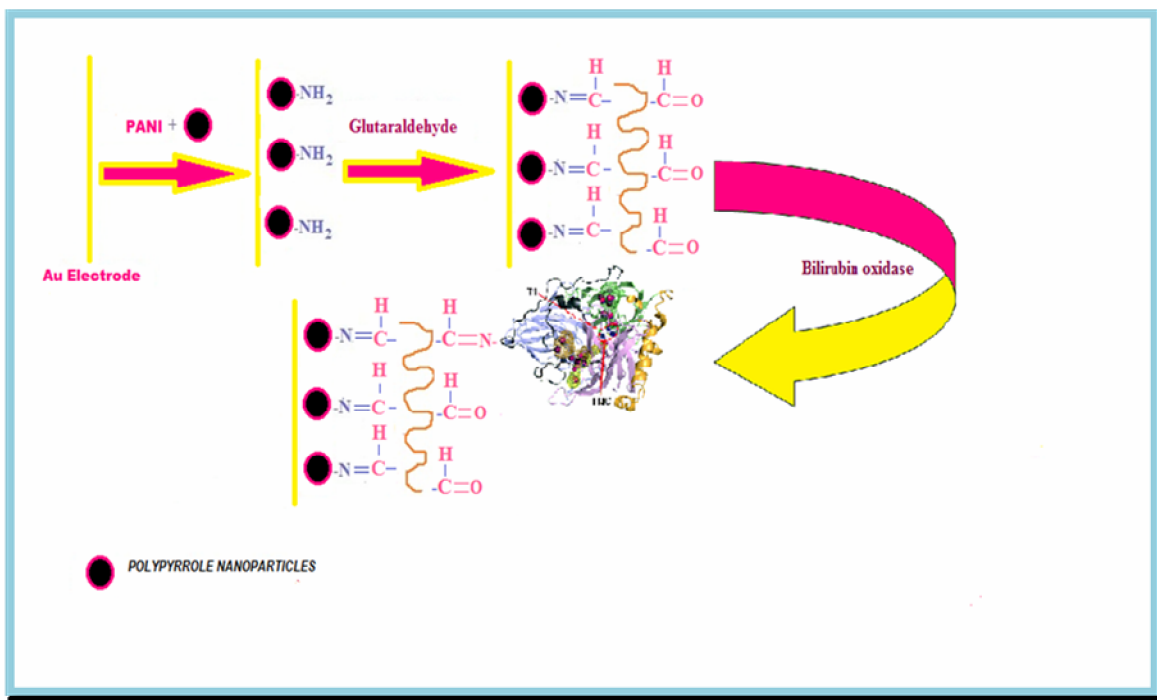


Fig.8 Cyclic voltamogram for (a) Bare Au (b) BOx/PANI/Au electrode (c) BOx/PpyNPs/PANI/Au electrode in 25 ml 0.05 Tris buffer with 9.0 pH containing 100 μ l bilirubin (0.5 mM); Scan rate: 20 mV/s

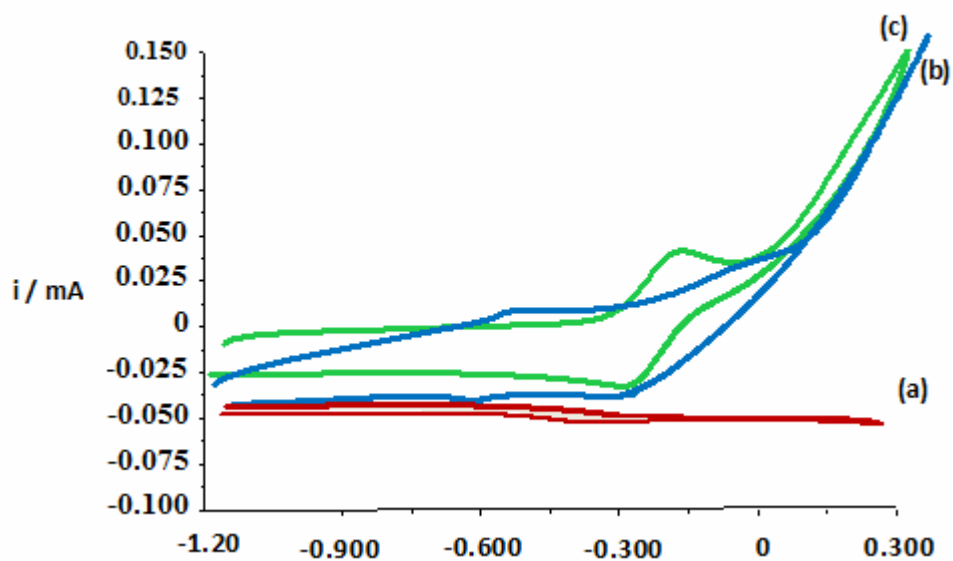


Fig.9 Cyclic voltammetry response of BOx/PpyNPs/PANI/Au electrode at the different potential in 25 ml 0.05 Tris buffer with 9.0 pH containing 100 μ l (0.5mM) bilirubin at a scan rate of 20 mV/s

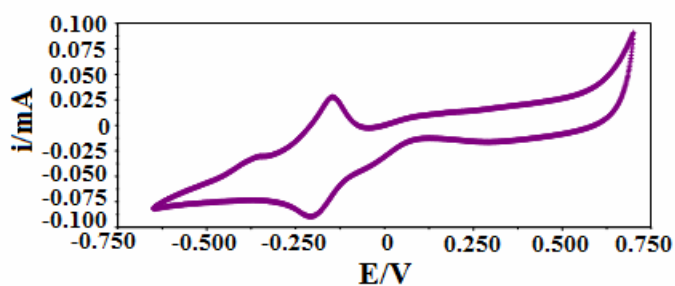
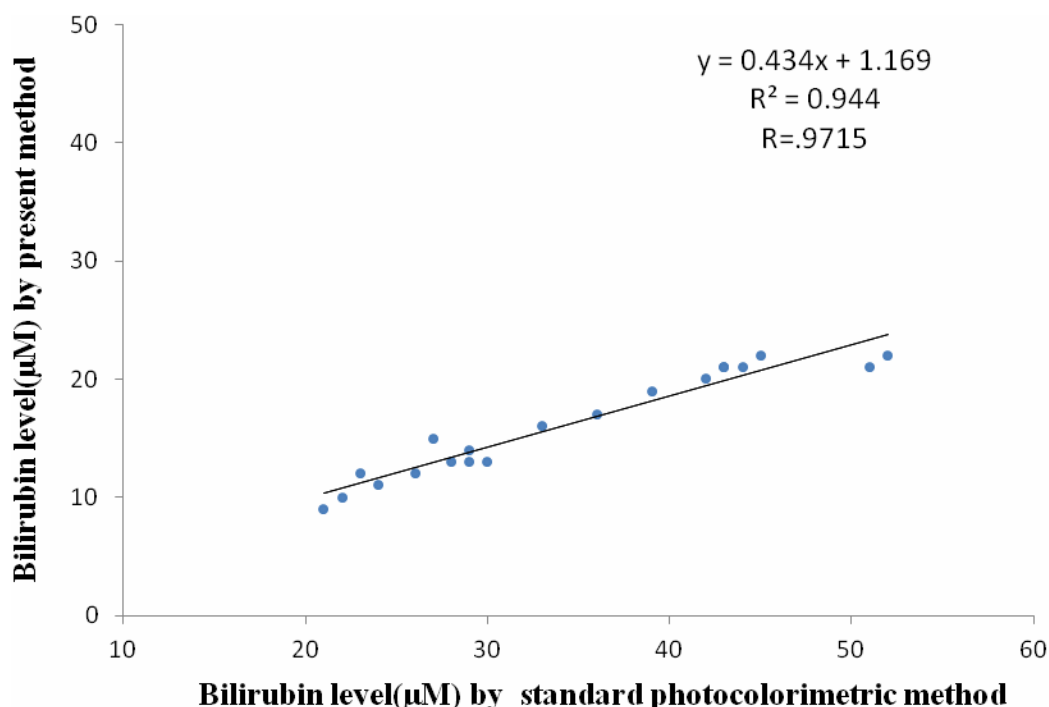


Fig.10. Correlation between serum bilirubin values measured by chemical photocolorimetric method (x axis) and the current method (y axis) employing the bilirubin biosensor based on PPyNPs/PANI/Au composite film



Acknowledgement

One of the author (Namita Malik) is thankful to Dr. Geeta Singh, DCRUST, Sonapat (Murthal) for allowing her to carry this research work in the laboratory of corresponding author.

References

Bais, R., Potezny, N., Edward, J.B., Rofe, A. M., Conyer, R., 1980. Oxalate determination by immobilized oxalate oxidase in a continuous flow system. *Anal. Chem.* 52, 508-511.

Bregmeyer, H.U., Horder, M., Rej, R., 1985. Approved recommendation on IFCC methods for the measurement of catalytic concentration of enzymes. *J Clin Chem Biochem.* 24, 481-489.

Doumas, B.T., Perry, B.W., Sasse, E. A.,

Straumfjord, J.V., 1973. Standardization in bilirubin assays: Evaluation of selected methods and stability of bilirubin solutions. *Clin. Chem.* 19, 984-993.

Fortuney, A., Guilbault, G., 1996. Enzyme electrode for the determination of bilirubin. *Electroanalysis.* 8, 229-232.

Klemm, J., Prodromidis, M., Karayannis, M., 2000. An enzymic method for the determination of bilirubin using an oxygen electrode. *Electroanalysis.* 12, 292-295.

Koch, T.R., Oakingbe, 1981. Feasibility of measuring free and total bilirubin electrochemically in serum. *Clin. Chem.* 27, 1295-1299.

Li, X. P., Rosenzweig, Z., 1997. A fiber optic sensor for rapid analysis of bilirubin in serum. *Anal. Chim. Act.* 353, 263-273.

- Maisels, M. J., 2009. Neonatal hyperbilirubinemia and kernicterus - not gone but sometimes forgotten. *Early Hum. Dev.* 85, 727-732.
- Malhotra, B. D., Chaubey A., 2003. Biosensors for clinical diagnostics industry. *Sens. Actu. B: Chem.* 91, 117-127.
- Michira, I., Akinyeye, R., Somerset, V., Klink, M. J., Sekota, M., Al-Ahmed, A., Baker, P. G. L., Iwuoha, E., 2007. Synthesis, Characterisation of Novel Polyaniline Nanomaterials and Application in Amperometric Biosensors. *Macromol. Symp.* 255, 57-69.
- Rahmana, M., Lee, A.K.S., Park, D.S., Won, M. S., Shima, Y. B., 2008. An amperometric bilirubin biosensor based on a conductive polyterthiophene-Mn(II) complex. *Biosens. Bioelectron.* 23, 857-864.
- Reung-u-Rai, A., Prom-jun, A., Prissanaroon-Ouajai, W., Ouajai, S., 2008. Synthesis of Highly Conductive Polypyrrole Nanoparticles via Microemulsion Polymerization. *JOM*, 18, 27-31
- Sherwin, J.E., Obernolte, R., 1989. *Bilirubin in Clinical chemistry: theory, analysis, and correlation*, second ed., St. Louis: The C.V. Mosby Company.
- Teles, F.R.R., Fonseca, L.P., 2008. Applications of polymers for biomolecule immobilization in electrochemical biosensors. *Mater. Sci. Engg.* 28, 1530-1543.
- Tiwari, D.C., Jain, R., Sharma, S., 2007. Electrochemically deposited polyaniline/polypyrrole polymer film modified electrodes for determination of furazolidone drug. *JSIR* 66, 1011-1018.
- Wang, C., Wang, G., Fang, B., 2009. Electrocatalytic oxidation of bilirubin at ferrocene carboxamide modified MWCNT-gold nanocomposite electrodes. *Microchim. Acta.* 164, 113-118.
- Wang, J., 2005. Nanomaterial-based electrochemical sensors. *Analyst* 130, 421-426.
- Wang, J., Ozsoz, M., 1990. A polishable amperometric biosensor for bilirubin. *Electroanalysis.* 2, 647-650
- Yang, Z., Zhang, C., 2011. Molecularly imprinted hydroxyapatite thin film for bilirubin recognition. *Biosens. Bioelectron.* 29, 167-171.
- Zhao, Z., Jiang, H., 2010. *Enzyme-based Electrochemical Biosensors*, China; Pier Andrea Serra (Ed.).